Manufacturing of metal-organic framework monoliths and their application in CO_2 adsorption

Wan Yun Hong[a,1], Semali P. Perera[a], Andrew D. Burrows[b]

[a] *Department of Chemical Engineering, University of Bath, Bath BA2 7AY, UK*

[b] *Department of Chemistry, University of Bath, Bath BA2 7AY, UK*

ABSTRACT

An important class of novel mesoporous and microporous adsorbents like metalorganic frameworks (MOFs) are normally produced in powder form. This paper presents a generic method of manufacturing and characterisation of these materials into low pressure drop and energy saving monolithic structures for industrial applications. One of the MOF candidates that was considered in this study was MIL-101 (Cr), and the model contaminant gas tested was carbon dioxide (CO_2). MIL-101 (Cr) monoliths were manufactured by paste extrusion techniques from the synthesized MIL-101 (Cr) powder. These MIL-101 (Cr) monoliths were then characterised using powder X-ray diffraction (PXRD), scanning electron microscopy (SEM), mercury intrusion porosimetry (MIP), radial compression tests and intelligent gravimetric analysis (IGA). Adsorption properties of the prepared MIL-101 (Cr) powder and monoliths were determined from their pure CO_2 sorption isotherms and dynamic adsorption breakthrough curves, that were carried out using high concentration (40% v/v) CO_2 challenge. Results have demonstrated that the resulting MIL-101 (Cr) monoliths were highly porous, mechanically strong on compressive loading, thermally regenerable with comparable CO_2 adsorption capacity to the synthesized MIL-101 (Cr) powder. From breakthrough curves, mass transfer characteristics such as mass transfer zone velocity and length of the prepared MIL-101 (Cr) monoliths have also been evaluated in this study.

Keywords:

MIL-101 (Cr), Metal-organic framework, Monoliths, CO_2 adsorption, Breakthrough curves

1 Introduction

New porous materials such as metal-organic frameworks (MOFs) have attracted a great deal of research interest, particularly in gas adsorption applications due to their large pore size [1], high porosity [2], large surface area [1-4], thermal and chemical stabilities [1, 4], adsorption capacity [1, 5, 6] and low density [3]. Their three-dimensional crystalline structures are built from metal ions or metallic clusters and organic linkers. A conventional method for synthesizing MOFs is by solvothermal reaction, which normally produced fine-particle powders [7]. For these MOFs powders to be applicable industrially, they need to be converted into a structure, which could be in the form of monoliths, beads, pellets, foams, etc. The most economical and energy efficient structure for use in any adsorption systems could be in the form of monoliths because its structure has low pressure drop and high mass transfer rates compared to other structures [8-11]. Experimental studies on MOFs for adsorption processes are mostly performed using its powder form and the generation of structured MOFs, particularly monolithic structure for industrial adsorption processes is rare. The fabrication of MOFs monoliths was first reported by Küsgens et al. [12] and they found that the *in situ* synthesis of a well-known MOF, i.e. copper (II) benzene-1,3,5-tricarboxylate [$Cu_3(BTC)_2$] on cordierite monoliths have low achievable adsorption capacity than manufacturing pure MOF monoliths. Although it is possible to manufacture pure $Cu_3(BTC)_2$ monoliths, their application for carbon dioxide (CO_2) adsorption in humid conditions is not sustainable because $Cu_3(BTC)_2$ has a poor hydrothermal stability, as proven by Liu et al. [13].

The manufacturing of MOFs monoliths from the powder form and their use in gas adsorption processes, particularly for biogas upgrading application, will be presented in this paper. The contaminant/adsorbate gas to be studied in this paper was CO_2 of high concentration, i.e. 40% (v/v); the typical CO_2 content found in biogas. One of the MOFs that was selected as a model adsorbent material for this study was MIL-101 (Cr). MIL-101 (Cr) was chosen because it is a stable adsorbent material under ambient atmosphere (for months) and even in the presence of various organic solvents and/or water [1]. Several studies [1, 14, 15] have demonstrated that MIL-101 (Cr) has a high adsorption capacity for carbon dioxide (CO_2); from 22.90 mmol g^{-1} at 25°C and 30 bar [16] up to 40 mmol g^{-1} at 25°C and 500 bar [17]. Other properties of MIL-101 (Cr) that need to be considered when developing a structured adsorbent for industrial applications with efficient adsorption performance are their pore properties and thermal stability. MIL-101 (Cr) has large pore sizes, ranging from 2.90 nm to 3.40 nm [1], large Langmuir surface area (using nitrogen isotherms) of 5900 ± 300 m^2 g^{-1} [1] and it is thermally stable up to 275°C [1, 15].

The process of manufacturing MIL-101 (Cr) monoliths by paste extrusion techniques will be described in this paper. Physical (crystal structure, surface morphology, pore structure and mechanical strength) and adsorptive properties (CO_2 sorption isotherms and adsorption breakthrough curves) of these MIL-101 (Cr) monoliths will then be characterized using powder X-ray diffraction (PXRD), scanning electron microscopy (SEM), mercury intrusion porosimetry (MIP), radial compression strength testing, intelligent gravimetric analysis (IGA) and dynamic adsorption flow breakthrough experiments. The aim of this paper is to show that MIL-101 (Cr) powder can be made into monolithic structure that is porous, mechanically strong on radial compression loading, thermally stable after adsorption-regeneration cycles

and could be used as a low pressure drop sorption device for adsorbing high concentration of CO_2 from gas streams.

2 Experimental

2.1 Materials

Chromium (III) nitrate nonahydrate (99%) and 1,4-benzenedicarboxylic acid (commonly known as terephthalic acid) (≥ 99%) were purchased from Acros Organics (UK), ethanol (≥ 99.8%) was purchased from Sigma-Aldrich Co. (USA), bentonite clay was purchased from Bath Potters' Supplies Ltd. (UK) and mercury was purchased from Fisher Scientific (UK). The adsorbate gas for adsorption experiments was CO_2 with a concentration of 40% (v/v) in air and it was purchased from BOC Ltd. (UK). All chemicals and gas were used as obtained from commercial sources, without further purification.

2.2 Synthesis of MIL-101 (Cr) powder

MIL-101 (Cr) powder was prepared by the modification of the synthesis described by Bromberg et al. [18], which eliminates the use of the toxic and highly corrosive hydrofluoric acid in the reaction. A mixture of chromium (III) nitrate (1.05 g), 1.4-benzendicarboxylic acid (0.40 g) and distilled water (12.25 g) was placed in an autoclave and heated to 220°C for 8 h. The autoclave was then cooled to room temperature. Insoluble green crystals of MIL-101 (Cr) were collected by centrifugation, washing with distilled water and dried at room temperature. As-synthesized MIL-101 (Cr) powder was then obtained.

2.3 Purification of MIL-101 (Cr) powder

The prepared as-synthesized MIL-101 (Cr) powder was treated with ethanol at 80°C for 4 h. Purified green crystals of MIL-101 (Cr) were then collected by centrifugation, washing with ethanol and dried at room temperature. The resulting product obtained was purified MIL-101 (Cr) powder.

2.4 Preparation of MIL-101 (Cr) monoliths

MIL-101 (Cr) monoliths were prepared by paste extrusion techniques from its as-synthesized and purified powders. The binding agent that was used in this work was bentonite clay. Green MIL-101 (Cr) powder, bentonite clay and water were mixed together to form a paste and allowed to matured at room temperature. When the MOF paste has matured into a workable paste, it was extruded into monolith on a single screw extruder. Extruded MOF monoliths were dried in a temperature controlled chamber at 10°C for several days before they were fired in a kiln at 150°C for about 33 h to form a strong and solid monolithic structure. Fired MIL-101 (Cr) monoliths were cut into 7.00 cm lengths for the dynamic adsorption breakthrough study. MIL-101 (Cr) monoliths containing 60% (w/w) of as-synthesized MIL-101 (Cr), 60% (w/w) and 75% (w/w) of purified MIL-101 (Cr) were prepared. All MIL-101 (Cr) monoliths that were prepared using this procedure have square channels with equal wall thickness, t_w, and channel size, d_c, of 0.90 mm.

2.5 Characterisation of MIL-101 (Cr) powder and monoliths

Powder and monolith samples of the as-synthesized and purified MIL-101 (Cr) were analysed by PXRD on a Bruker AXS D8 Advance diffractometer with copper radiation in 2θ angles ranging from 3° to 40°. Surface morphologies of the as-synthesized and purified MIL-101 (Cr) powder and monolith was examined by SEM using a JEOL JSM-6480 LV microscope, in which the samples were coated with a thin layer of gold using Edwards S150B sputter coater. Pore structures of the as-synthesized and purified MIL-101 (Cr) powder and monoliths were characterized by MIP on Micromeritics AutoPore III, where mercury was forced into the pores of the test samples at elevated pressures. Mechanical radial compression strengths of the 60% (w/w) and 75% (w/w) purified MIL-101 (Cr) monoliths were determined by performing radial compression tests on the Instron 3369 Universal Tester machine with a compression rate of 0.50 mm min^{-1}.

2.6 Adsorption properties of MIL-101 (Cr) powder and monoliths

Pure CO_2 sorption properties of purified MIL-101 (Cr) powder and monolith (containing 60% (w/w) MIL-101 (Cr) and 40% (w/w) binder) were evaluated using its sorption isotherms for pressure ranging from 0 bar to 4.50 bar at 20°C and 25°C on the Hiden intelligent gravimetric analyser. Meanwhile, the dynamic adsorption of CO_2 on MIL-101 (Cr) monoliths was investigated on an adsorption flow-breakthrough apparatus. The apparatus consists of a feed gas flow system, an adsorption column and an effluent gas analytical system, as illustrated in Fig. 1. Prior to the start of the adsorption experiments, all test samples were regenerated at 150°C for at least 12 h.

Regenerated MIL-101 (Cr) monoliths with a length of 7.00 cm and a diameter of 21.47 mm was packed tightly and held in the centre of the steel tubular adsorption column by wrapping the inlet end of the monolith with PTFE gas sealant tape and a nitrile O-ring so that the feed gas only flows through the monolith channels and not around the monolith wall. A flow distributor was placed on the inlet end of the adsorption column to ensure uniform gas flow through the monolith channels. The packed adsorption column was mounted vertically on the adsorption flow-breakthrough apparatus. In this study, CO_2 gas with a concentration of 40% (v/v) was used as the feed adsorbate gas and compressed air was used as the purging gas for cleaning the lines of the adsorption system. All adsorption experiments were performed with a feed gas flow rate of 500 mL min^{-1} with an absolute pressure of 2 bar under ambient temperature.

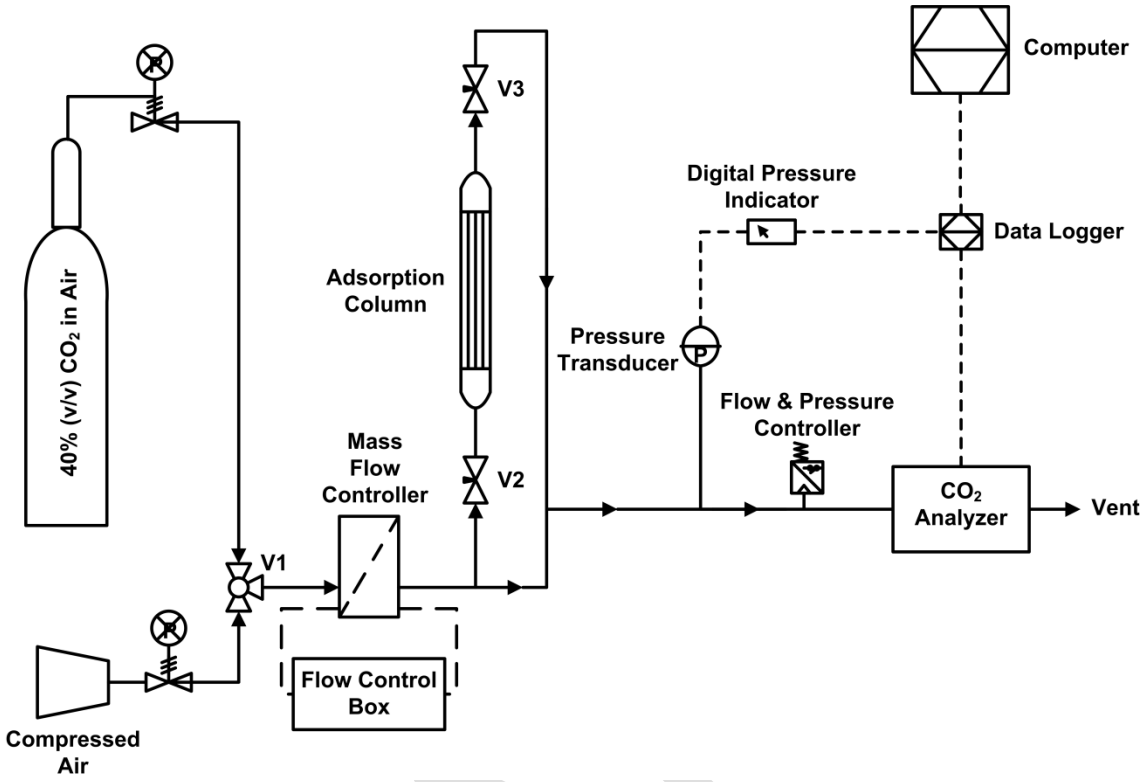

Fig. 1. Schematic flow diagram of the adsorption flow-breakthrough apparatus.

Adsorption breakthrough curves generated from the adsorption experiments were used to determine dynamic (such as breakthrough time, stoichiometric time, equilibrium time and equilibrium adsorption capacity, mass transfer zone (MTZ) velocity and length) adsorption properties of the test samples. The breakthrough time, t_b, is the time at which the effluent gas concentration starts to increase by about 10% of the feed gas concentration (i.e. $\frac{C}{C_0} \geq$ 0.10) and the equilibrium time, t_e, is the time at which the effluent gas concentration is the same as the feed gas concentration (i.e., $\frac{C}{C_0}$ = 1.00). Both the breakthrough and equilibrium times were obtained directly from the adsorption breakthrough curve whereas the stoichiometric time, t_s, was determined by equating the area under the breakthrough curve after t_b (represented by area A) and the area above the breakthrough curve before t_e (represented by area B), see Fig. 2.

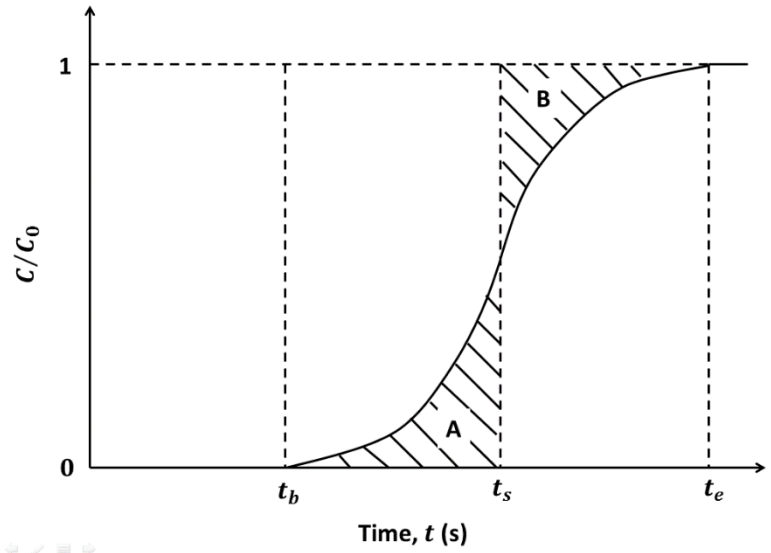

Fig. 2. Typical breakthrough curve.

The equilibrium adsorption capacity of the adsorbent material, $\bar{q}_{eq}$ (millimole of CO_2 being adsorbed per gram of MIL-101 (Cr) adsorbent), was calculated using equation (1) [19]:

$$\bar{q}_{eq} = \frac{F}{m}\left(t_e - \sum_{t=0}^{t=t_e} \frac{C}{C_0} dt\right) \quad (1)$$

where F is the molar flow rate of the feed gas through the adsorbent bed (mmol s^{-1}), m is the mass of the adsorbent (g), t_e is the equilibrium time (s) C_0 is the concentration of the feed gas (g m^{-3}) and C is the concentration of the effluent gas (g m^{-3}) at time t (s). The velocity of the mass transfer zone, u_{MTZ} (millimetre of CO_2 being transported per second), and normalised length of the mass transfer zone, L_{MTZ} (millimetre of CO_2 being transported per millimetre of adsorbent bed), in the monolithic adsorbent bed were estimated using the following equations [20]:

$$u_{MTZ} = \frac{L}{t_s} \quad (2)$$

$$L_{MTZ} = \frac{u_{MTZ}(t_e - t_b)}{L} \quad (3)$$

where L is the length of the monolith (mm), t_s is the stoichiometric time (s) and t_b is the breakthrough time (s).

3 Results and discussion

3.1 Manufacturing of MIL-101 (Cr) monoliths from its synthesized powders

Fine green powders of as-synthesized and purified MIL-101 (Cr) were synthesized successfully in the laboratory. Production of sufficient amount of MIL-101 (Cr) powder for monolith manufacturing was found to be very challenging since its powder synthesis has a low product yield. Despite the low productivity of MIL-101 (Cr) powder, this study was able to manufacture MIL-101 (Cr) monoliths with high proportion of MIL-101 (Cr) for characterisation and adsorption studies. As-synthesized and purified MIL-101 (Cr) monoliths with square channels containing 60% (w/w) and 75% (w/w) of MIL-101 were manufactured successfully from its respective powders without any defects or crack formation on the monolithic structure. As seen on the photograph of the fired MIL-101 (Cr) monolith in Fig. 3, the colour of the prepared MIL-101 (Cr) monoliths was green.

Fig 3 Cross-sectional view of a fired MIL-101 (Cr) monolith.

3.2 Physical characteristics of MIL-101 (Cr) powders and monoliths

PXRD patterns of the synthesized MIL-101 (Cr) powders and the prepared MIL-101 (Cr) monoliths that are shown in Fig. 4 have similar peak positions and they were consistent with that reported in the literature [1, 18]. This means that the crystal structure (shape and size) of the synthesized MIL-101 (Cr) powder was maintained in the fired monolithic structure and the MIL-101 (Cr) crystal has cubical cell with free aperture of approximately 8.90 nm, as claimed by Férey et al. [1]. The difference in diffraction peak intensities between the as-synthesized and purified MIL-101 (Cr) powders was due to the removal of unreacted 1,4-benzendicarboxylic acid from the pores of the MIL-101 (Cr) crystal. A significant change in peak intensities between the purified MIL-101 (Cr) powder and monolith was also seen in Fig. 4, which could be due to the presence of binding agent in the pores of the purified MIL-101 (Cr) crystals.

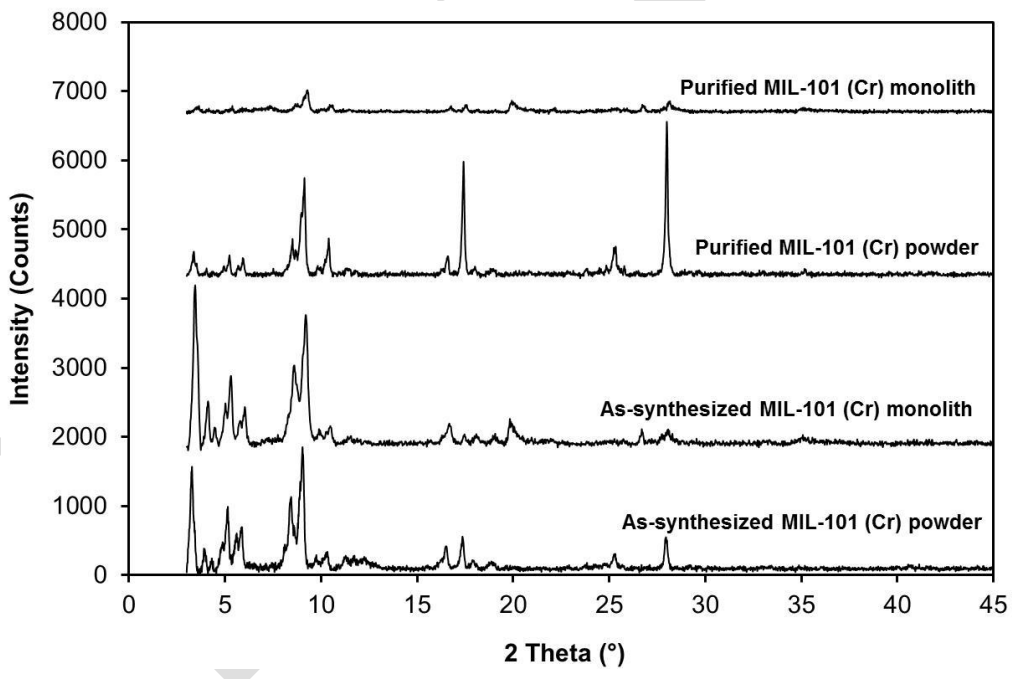

Fig. 4. PXRD pattern of the as-synthesized and purified MIL-101 (Cr) powders and its monoliths.

SEM images of as-synthesized MIL-101 (Cr) powder and monolith are given in Fig. 5 (a) and (b), respectively. These micrographs clearly show that the MIL-101 (Cr) crystals were cubical in structure and they were interlinked with the binder after the firing process. Similar

morphologies were expected for the purified MIL-101 (Cr) powder and monolith, as shown in Fig. 6 (a) and (b), respectively. Micrographs of the powdered MIL-101 (Cr) in Fig. 5 (a) for the as-synthesized MIL-101 (Cr) and in Fig. 6 (a) for the purified MIL-101 (Cr) shows that they have a particle size that ranges from 0.10 μm to 1 μm.

a)

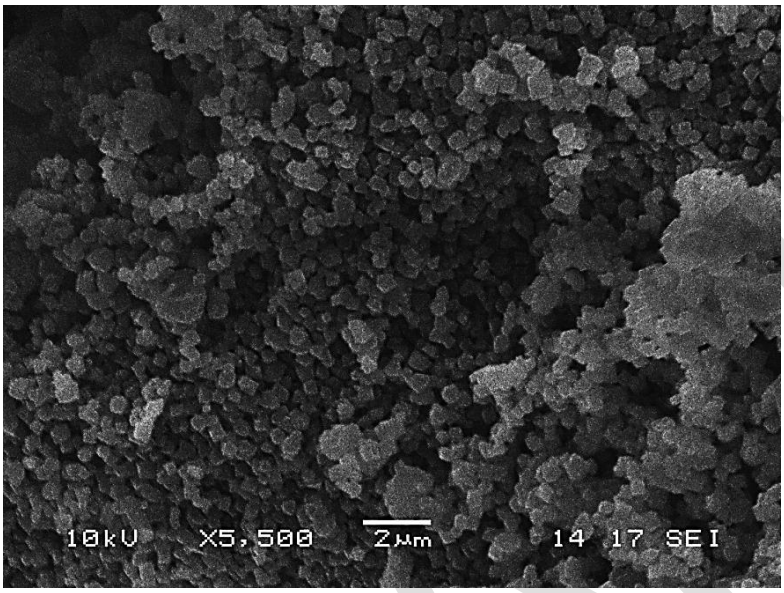

b)

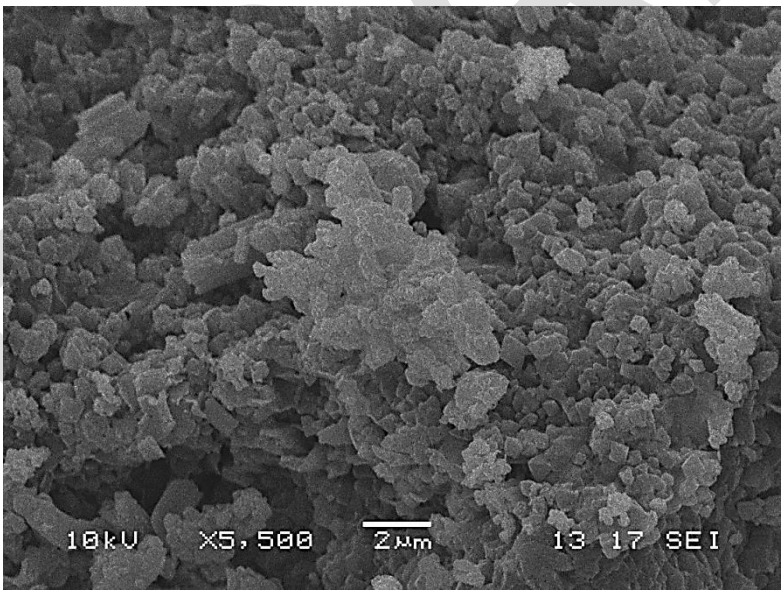

Fig. 5. Scanning electron micrograph of as-synthesized MIL-101 (Cr) (a) powder and (b) monolith.

Pore properties of as-synthesized and purified MIL-101 (Cr) powders and monoliths containing 60% (w/w) MIL-101 and 40% (w/w) binder are listed in Table 1. It can be seen

from their pore properties that the porosity of the purified MIL-101 (Cr) was lower (4.42% for powder and 17.93% for monolith) than that of the as-synthesized MIL-101 (Cr). The low porosity of the purified MIL-101 (Cr) powder indicates that the crystal structure of the as-synthesized MIL-101 (Cr) was changed when it was purified with hot ethanol, as confirmed by the difference in the locations of their PXRD peaks. Pore properties (such as total pore surface area, average pore diameter and porosity) of the as-synthesized and purified MIL-101 (Cr) powders were expected to be higher than their monoliths since they only contained pure MIL-101 (Cr) materials while their monoliths contained bentonite as the binder apart from the MIL-101 (Cr). As expected, the total pore surface area of the as-synthesized and purified MIL-101 (Cr) powders and monoliths obtained using MIP was lower than those published in the literature. The difference in total pore surface area between the MIL-101 (Cr) materials prepared in this study and that reported in the literature could be due to incomplete activation of MIL-101 (Cr) crystals, variation in synthesis methods or MIL-101 (Cr) crystals and the characterisation techniques (surface area and pore measurements using nitrogen adsorption isotherms) used. The presence of bentonite in the monolithic structure also caused the bulk density of the prepared MIL-101 (Cr) monoliths to be denser than the synthesized MIL-101 (Cr) powders.

Elastic moduli of 60% (w/w) and 75% (w/w) MIL-101 (Cr) monoliths on radial compression were found to be 10.60 N mm^{-2} and 4.97 N mm^{-2}, respectively. These compression results demonstrate that a high proportion of binder in the MIL-101 (Cr) monolith will produce a mechanically strong monolithic structure.

(a)

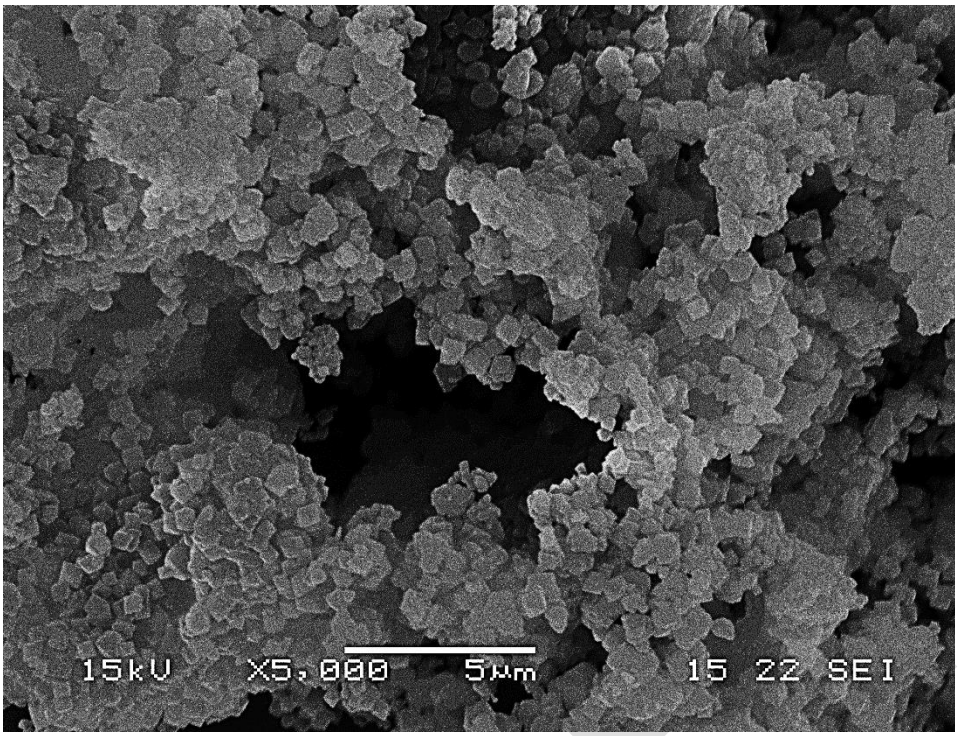

(b)

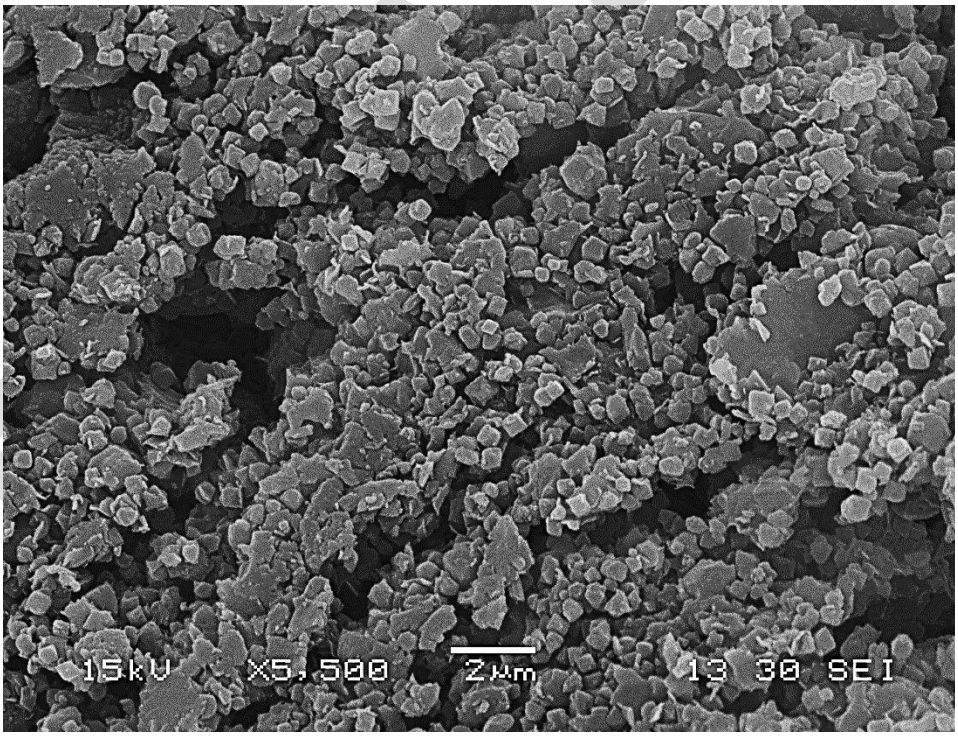

Fig. 6. Scanning electron micrograph of purified MIL-101 (Cr) (a) powder and (b) monolith.

Table 1

Pore properties of as-synthesized and purified MIL-101 (Cr) powders and monoliths (containing 60% MIL-101 (Cr) and 40% binder; in w/w).

Pore properties of MIL-101 (Cr)	As-synthesized		Purified	
	Powder	Monolith	Powder	Monolith
Total intrusion volume (mL g^{-1})	2.89	1.14	2.21	0.71
Total pore surface area (m^2 g^{-1})	345.49	229.42	202.22	182.84
Average pore diameter (nm)	33.50	19.90	43.60	15.60
Bulk density (g mL^{-1})	0.28	0.60	0.35	0.79
Porosity (%)	79.83	68.59	76.30	56.29

3.3 Adsorption properties of MIL-101 (Cr) powder and monoliths

Pure CO_2 adsorption isotherms of purified MIL-101 (Cr) powder and monolith (containing 60% (w/w) MIL-101 (Cr) and 40% (w/w) binder) at 20°C and 25°C are given in Fig. 7. These CO_2 sorption isotherms showed that the adsorption capacity of CO_2 for the purified MIL-101 (Cr) monolith was lower than the purified MIL-101 (Cr) powder. This was due to the fact that the purified MIL-101 (Cr) monolith contained bentonite as a binding agent besides MIL-101 (Cr) while the purified MIL-101 (Cr) powder only contained pure MIL-101 (Cr). In this study, the adsorption capacity of CO_2 for the purified MIL-101 (Cr) powder at 2 bar and at 25°C was found to be reduced by 36.81% (from 1.44 mmol g^{-1} to 0.91 mmol g^{-1}) in comparison to that for the purified MIL-101 (Cr) monolith. The purified MIL-101 (Cr) monolith that was manufactured in this study contained 40% (w/w) binder and the reduction in adsorption capacity observed for the tested MIL-101 (Cr) monolith was acceptable. Most of the industrial standard adsorbents would have 15% (w/w) to 20% (w/w) binder content,

which will cause the adsorption capacity of the adsorbent to be decreased to a certain extent.

The effect of pressure (up to 4.50 bar), temperature and repeatability of the adsorption run on the adsorption capacity of CO_2 for the purified MIL-101 (Cr) monolith and powder was also shown by their CO_2 sorption isotherms in Fig. 7. As expected, the adsorption capacity of CO_2 for the purified MIL-101 (Cr) monolith and powder increases with increasing pressure but decreases with increasing temperature. The second adsorption run showed a slight decrease in CO_2 adsorption capacity. Although this paper mainly concentrates on low pressure adsorptive separations (at 2 bar), much greater CO_2 adsorption capacity could be achieved when the MIL-101 (Cr) monolithic adsorption system was operated at higher pressures. It has been reported in the literature that MIL-101 (Cr) has high CO_2 adsorption capacity, from 22.90 mmol g^{-1} at 30 bar up to 40 mmol g^{-1} at 500 bar at 25°C [16, 17].

Dynamic adsorption properties of the prepared MIL-101 (Cr) monoliths are summarised in Table 2. Adsorption breakthrough curves for 40% (v/v) CO_2 on as-synthesized and purified MIL-101 (Cr) monoliths are compared in Fig. 8. Results from the adsorption experiments showed that the equilibrium adsorption capacity of CO_2 molecules on the MIL-101 (Cr) crystals was increased by approximately 38.30% (from 1.41 mmol g^{-1} to 1.95 mmol g^{-1}) when the as-synthesized MIL-101 (Cr) was purified to remove unreacted 1,4-benzenedicarboxylic acid from the pores of the MIL-101 (Cr) crystals.

On the other hand, the equilibrium adsorption capacity of CO_2 for purified MIL-101 (Cr) monoliths with different weight percentages of purified MIL-101 (Cr) in the monolithic structure did not show the expected improvement in CO_2 adsorption, i.e. a drop of 30.26% in equilibrium adsorption capacity of CO_2 (from 1.95 mmol g^{-1} to 1.36 mmol g^{-1}), when the

content of purified MIL-101 (Cr) in the monolithic structure was increased from 60% (w/w) to 75% (w/w), as presented in Fig. 9. The reason for this was probably due to the manufacturing effects (such as inconsistency when mixing the dry powder and/or the maturity of the adsorbent paste) of the purified MIL-101 (Cr) monoliths that resulted in more active sites of the adsorbent being blocked by the binder material on the 75% (w/w) purified MIL-101 (Cr) monolith than that on the 60% (w/w) purified MIL-101 (Cr) monolith. The 75% (w/w) purified MIL-101 (Cr) monolith showed a longer time to reach equilibrium (t_e = 499 s), indicating that the mass transfer resistance of this monolith was higher compared to the 60% (w/w) purified MIL-101 (Cr) monolith (t_e = 228 s).

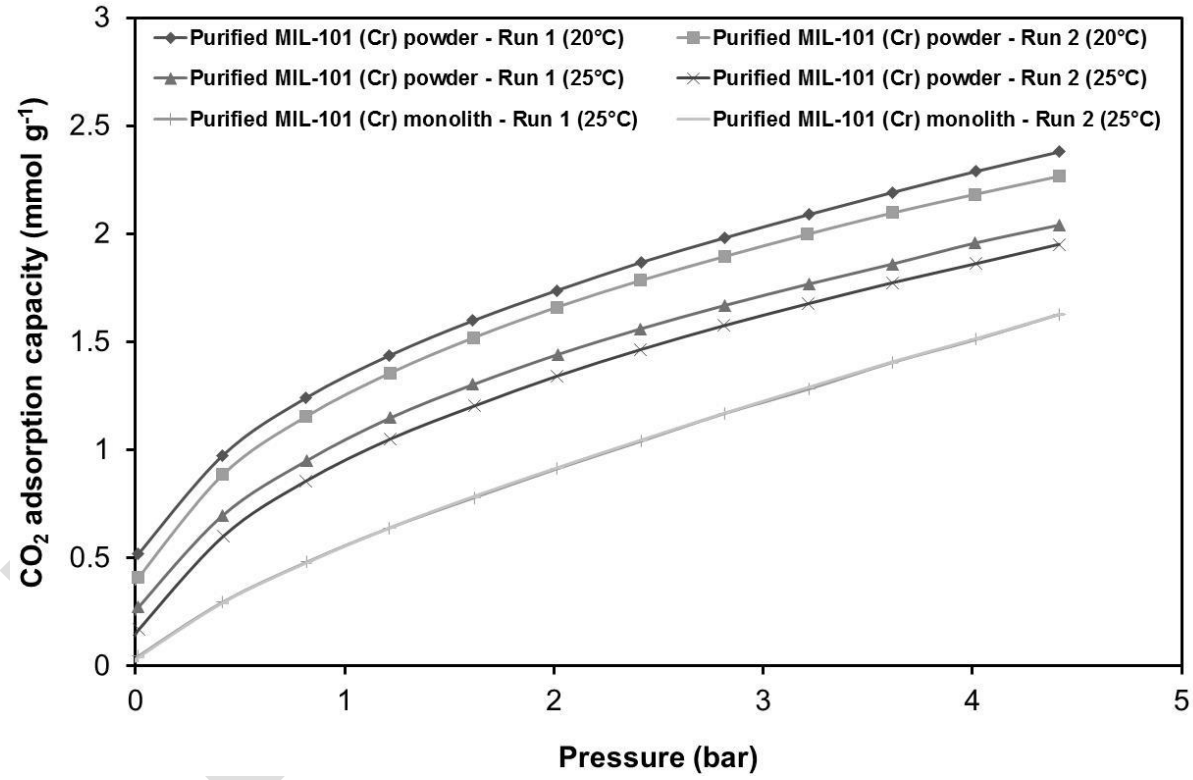

Fig. 7. CO_2 sorption isotherms of purified MIL-101 (Cr) powder and monolith (with 60% (w/w) purified MIL-101 (Cr):40% (w/w) binder) at 20°C and at 25°C.

Table 2

Adsorption properties determined using adsorption breakthrough data for as-synthesized and purified MIL-101 (Cr) monoliths with 40% (v/v) CO_2 at 2 bar.

MIL-101 (Cr) monoliths	As-synthesized	Purified	
MIL-101 (Cr):binder (% w/w)	(60:40)	(60:40)	(75:25)
Mass of MIL-101 (Cr) adsorbent (g) in sample, m	8.21	3.43	8.28
Breakthrough time, t_b (s)	50	42	54
Stoichiometric time, t_s (s)	97	65	96
Equilibrium time, t_e (s)	629	228	499
Amount of CO_2 adsorbed, q_{eq} (mmol)	11.57	6.67	11.29
Equilibrium adsorption capacity of CO_2, $\bar{q}_{eq}$ (mmol g^{-1})	1.41	1.95	1.36
MTZ velocity, u_{MTZ} (mm s^{-1})	0.08	0.05	0.08
MTZ length, L_{MTZ} (mm mm^{-1})	0.53	0.40	0.48

Good repeatability of experimental adsorption data was also shown by the prepared MIL-101 (Cr) monoliths, as illustrated in Fig. 10. Comparison on the adsorption capacity of CO_2 obtained from IGA and adsorption flow breakthrough experiments, i.e. at 2 bar, revealed that there was a slight variation in the value of the CO_2 adsorption capacity for the purified MIL-101 (Cr) monoliths and this could be due to experimental error. From the CO_2 adsorption breakthrough curves of the tested MIL-101 (Cr) monoliths, the mass transfer zone velocities and lengths were calculated and are given in Table 2.

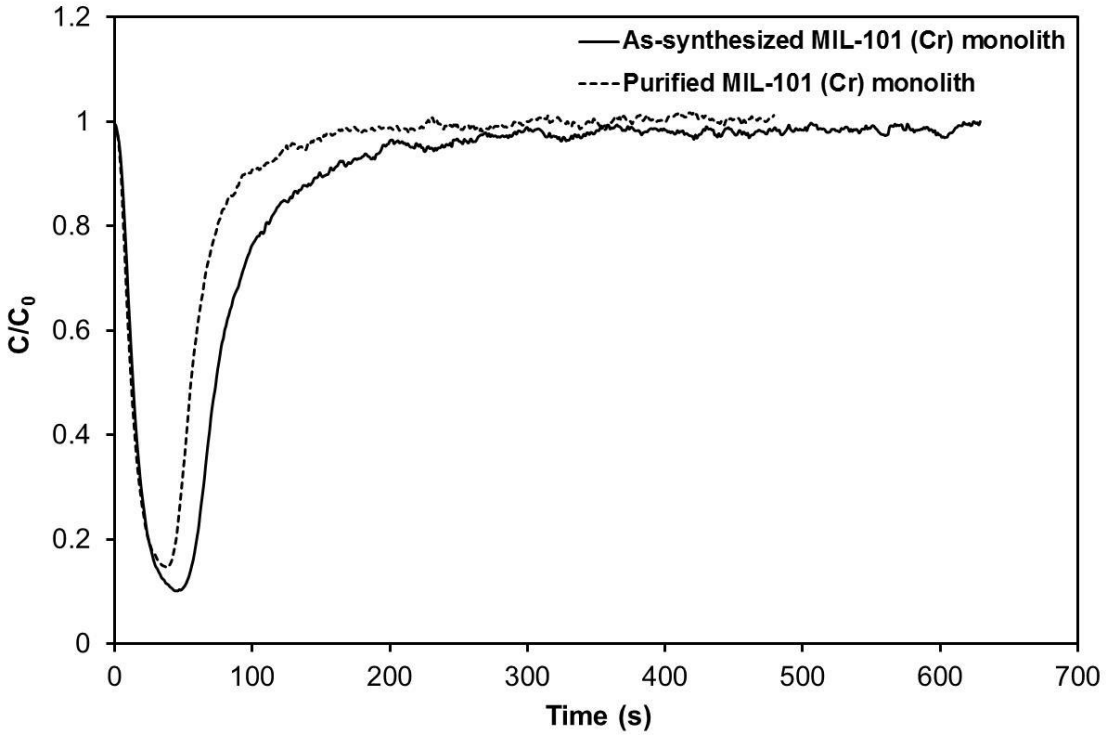

Fig. 8. Dynamic adsorption of 40% (v/v) CO_2 on 60% (w/w) as-synthesized and purified MIL-101 (Cr) monoliths and purified MIL-101 (Cr) powder.

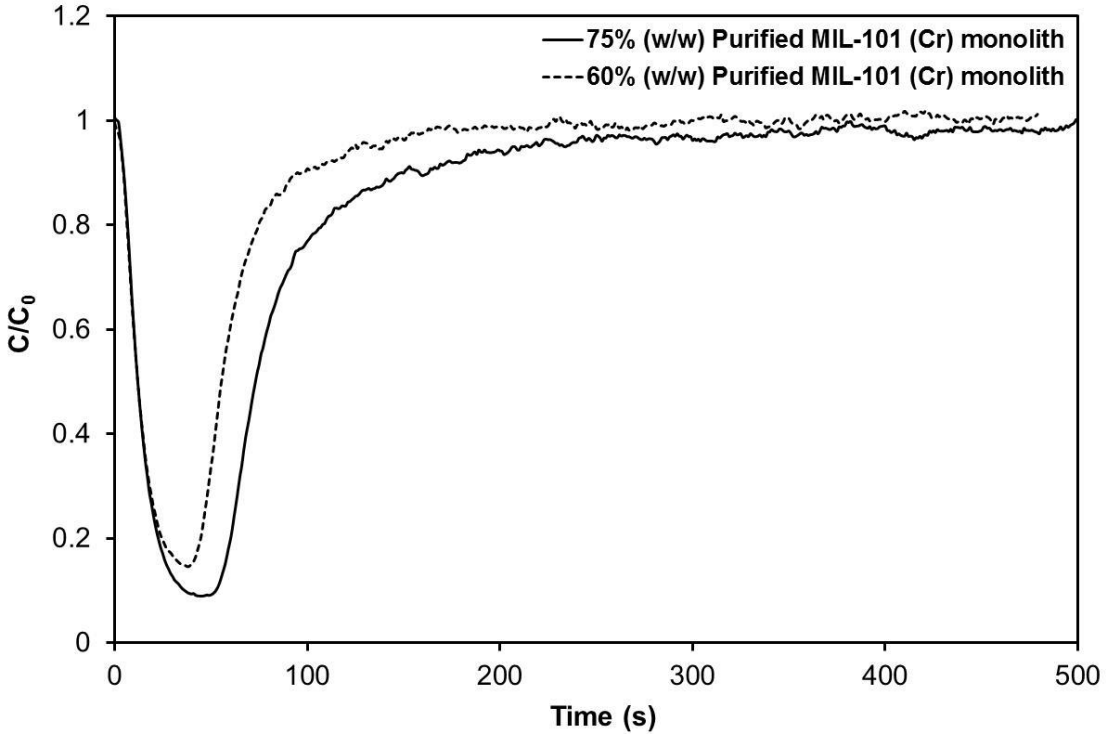

Fig. 9. Dynamic adsorption of 40% (v/v) CO_2 on 60% (w/w) and 75% (w/w) purified MIL-101 (Cr) monoliths.

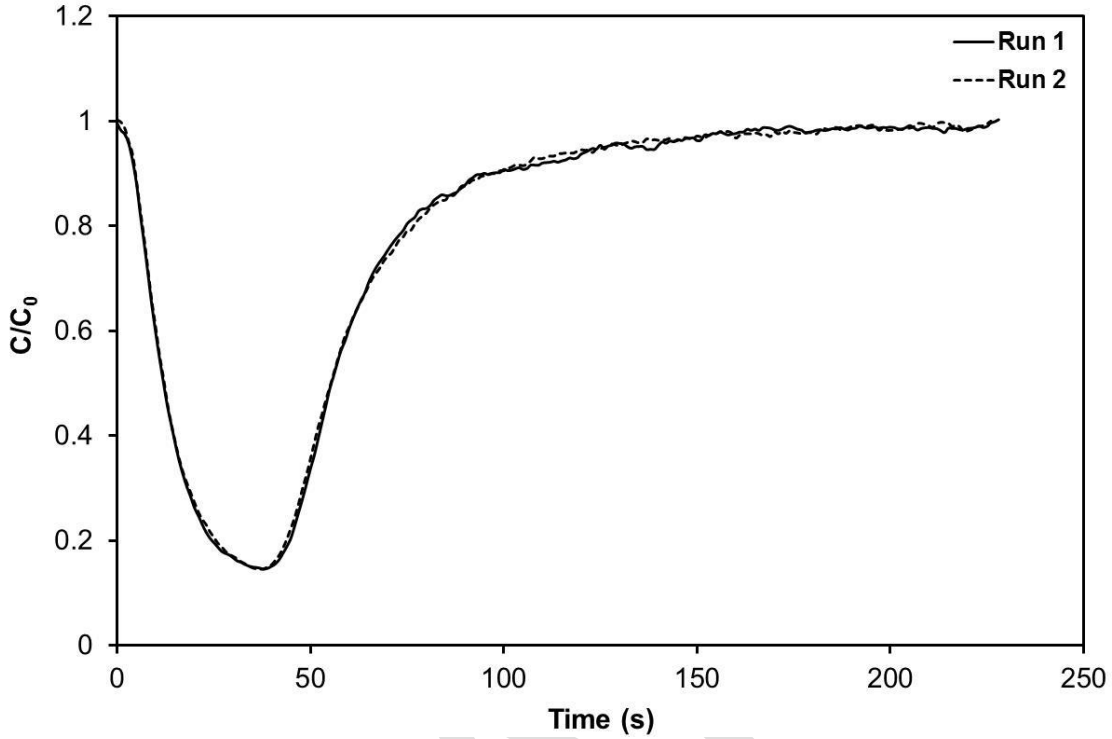

Fig. 10. Dynamic adsorption of 40% (v/v) CO_2 on 60% (w/w) purified MIL-101 (Cr) monolith with repeated runs.

Dynamic breakthrough studies are important for adsorption separation processes since the mass transfer zone velocity indicates how fast the adsorption concentration front moves through the adsorbent bed while the mass transfer zone length indicates the distance of the adsorbent bed being utilised by the CO_2 molecules.

4 Conclusions

In conclusion, highly porous MIL-101 (Cr) monoliths have been successfully manufactured in this study. As indicated by the pure CO_2 sorption isotherms for the purified MIL-101 (Cr) powder and monolith, adsorption system with enhanced adsorption capacity of CO_2 could be achieved when it was operated at higher pressure and at reduced temperature. Adsorption flow breakthrough experiments have demonstrated that MIL-101

(Cr) monoliths can be regenerated at a moderate temperature of 150°C for repeated adsorption runs without loss of performance. MIL-101 (Cr) was found to have a high CO_2 equilibrium adsorption capacity when it was purified. The velocity and length of the mass transfer zone for the prepared MIL-101 (Cr) monolith have also been evaluated from its CO_2 adsorption breakthrough curves. This study proved the possibility of developing porous and regenerative metal-organic framework monolithic structure that can be used in industrial applications for adsorbing high concentration of CO_2 gas.

Acknowledgements

The authors gratefully acknowledge the Brunei Government for providing the financial supports of this research to Ms Wan Yun Hong. Technical assistances from Mrs Ursula Potter on SEM characterisation at Microscopy and Analysis Suite (MAS) and Dr Gabriel Kociok-Kohn on PXRD characterisation at Chemical Characterisation and Analysis Facility (CCAF), University of Bath were appreciated. Further thanks were also expressed to Dr Olivier Camus for general assistances and advices on laboratory research and Mr Andrew Physick for isotherm measurements.

References

[1] G. Férey, C. Mellot-Draznieks, C. Serre, F. Millange, J. Dutour, S. Surblé, I. Margiolaki, Science, 309 (2005) 2040-2042.

[2] H.K. Chae, D.Y. Siberio-Perez, J. Kim, Y. Go, M. Eddaoudi, A.J. Matzger, M. O'Keeffe, O.M. Yaghi, Nature, 427 (2004) 523-527.

[3] Y. Li, R.T. Yang, Langmuir, 23 (2007) 12937-12944.

[4] H. Li, M. Eddaoudi, M. O'Keeffe, O.M. Yaghi, Nature, 402 (1999) 276-279.

[5] A.R. Millward, O.M. Yaghi, Journal of the American Chemical Society, 127 (2005) 17998-17999.

[6] D. Britt, D. Tranchemontagne, O.M. Yaghi, Proceedings of the National Academy of Sciences, 105 (2008) 11623-11627.

[7] P.A. Wright, Microporous Framework Solids, Royal Society of Chemistry, Cambridge, 2008.

[8] F. Rezaei, P. Webley, Chemical Engineering Science, 64 (2009) 5182-5191.

[9] B. Crittenden, A. Patton, C. Jouin, S. Perera, S. Tennison, J. Echevarria, Adsorption, 11 (2005) 537-541.

[10] L.Y. Lee. Control of Volatile Organic Chemical Emissions by Adsorption onto Hydrophobic and Organophilic Adsorbents, PhD Thesis, University of Bath, 1997.

[11] Y.Y. Li. Air Separation with Monolithic Adsorbents, PhD Thesis, University of Bath, 1998.

[12] P. Küsgens, A. Zgaverdea, H.-G. Fritz, S. Siegle, S. Kaskel, Journal of the American Ceramic Society, 93 (2010) 2476-2479.

[13] J. Liu, Y. Wang, A.I. Benin, P. Jakubczak, R.R. Willis, M.D. LeVan, Langmuir, 26 (2010) 14301-14307.

[14] P. Küsgens, M. Rose, I. Senkovska, H. Fröde, A. Henschel, S. Siegle, S. Kaskel, Microporous and Mesoporous Materials, 120 (2009) 325-330.

[15] K. Munusamy, G. Sethia, D.V. Patil, P.B. Somayajulu Rallapalli, R.S. Somani, H.C. Bajaj, Chemical Engineering Journal, 195–196 (2012) 359-368.

[16] Z. Zhang, S. Huang, S. Xian, H. Xi, Z. Li, Energy & Fuels, 25 (2011) 835-842.

[17] Q. Liu, L. Ning, S. Zheng, M. Tao, Y. Shi, Y. He, Scientific Reports, 3 (2013).

[18] L. Bromberg, Y. Diao, H. Wu, S.A. Speakman, T.A. Hatton, Chemistry of Materials, 24 (2012) 1664-1675.

[19] J.D. Seader, E.J. Henley, Separation Process Principles, John Wiley, New York; Chichester, 1998.

[20] J.L. Kovach, in: P.A. Schweitzer (Ed.), Handbook of Separation Techniques for Chemical Engineers, 2nd ed, McGraw-Hill, New York; London, 1988.